MechSE

CCC Annual Report

UIUC, August 20, 2014

System of Models for Transient Multiphase Flow in UTN, Slide-gate, SEN, and CC mold

Rui Liu and BG Thomas

Department of Mechanical Science & Engineering
University of Illinois at Urbana-Champaign

Acknowledgments

- Continuous Casting Consortium Members (ABB, **ArcelorMittal**, Baosteel, Magnesita Refractories, Nippon Steel and Sumitomo Metal Corp., Nucor Steel, Postech/ Posco, Severstal, SSAB, Tata Steel, ANSYS/ Fluent)
- Also:
  - Blue Waters / National Center for Supercomputing Applications (NCSA) at UIUC
  - National Science Foundation Grant CMMI-11-30882
  - National Science Foundation Grant CMMI-13-00907

Problem Description

- **Target problem:**
  - **Model true transient multiphase flow**
- **Difficulties:**
  - **Gas injection**
    - Gas flow rate and distribution into UTN
    - Initial bubble size
  - **Flow rate variation during actuator movements**
  - **Validation of computational models**
- **Model system:**
  - **Flow rate models**
  - **Porous flow model**
  - **Free-surface tracking**
  - **Multiphase flow**

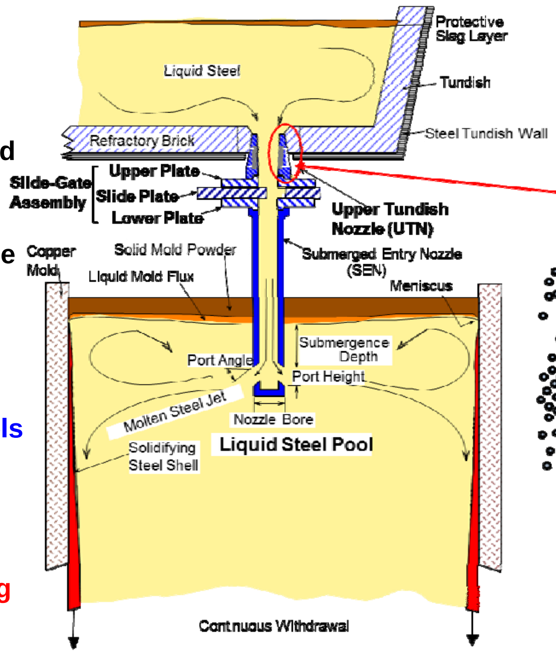

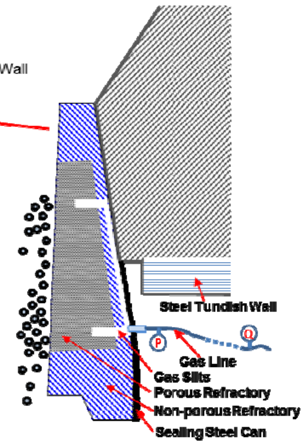

Models of Gas Flow Through Heated Porous Refractory (UTN)

Heat Conduction: $\nabla \cdot (k \nabla T) = 0$ **(1)**

Ideal Gas Law: $p = \rho R T$ **(2)**

Mass Conservation (or continuity): $\nabla \cdot (\rho \mathbf{v}) = 0$ **(3)**

Full Set of Navier-Stokes Equations for flow in porous media:

Porous-flow Model:

$$\frac{\partial(\rho \mathbf{v})}{\partial t} + \nabla \cdot (\rho \mathbf{v}\mathbf{v}) = -\nabla p + \nabla \cdot (\mu \nabla \mathbf{v}) + \mathbf{F} - \left(\frac{\mu}{\alpha} \mathbf{v} + C \frac{1}{2} \rho |\mathbf{v}| \mathbf{v} \right) \quad (4)$$

viscous resistance   inertial resistance

Darcy's Law: $\mathbf{v} = -K_D \nabla p$ **(5)**

Combining (1), (2), (3) and (5):

Pressure-source Model:

$$\nabla \cdot (K_D \nabla p) = -\frac{RT}{p} \left[\nabla \left(\frac{p}{RT} \right) \cdot (K_D \nabla p) \right] = \dot{S} \quad (6)$$

pressure diffusion   pressure source due to gas expansion

Permeability Variation

--Dependence of Permeability/Gas Viscosity on Temperature

Specific permeability, (from ArcelorMittal for MgO or Alumina refractory: $0.8 - 1.2 \times 10^{-12}\ m^2$

$$K_D = \frac{K_{DS}}{\mu(T)} \quad \begin{cases} K_{DS} = 1.01\times10^{-12} m^2 & \text{(constant specific permeability)} \\ \mu(T) & \text{(gas dynamic viscosity, as a function of local temperature)} \end{cases}$$

Viscosity Varying with Temperature:*

$$\mu(T) = \mu_0 * 10^{\left(0.63842\lg T - 6.9365/T - 3374.72/T^2 - 1.51196\right)}$$

$$\mu_0 = 2.228\times10^{-5}\ Pa\cdot s$$

Room temperature (20 C) argon viscosity

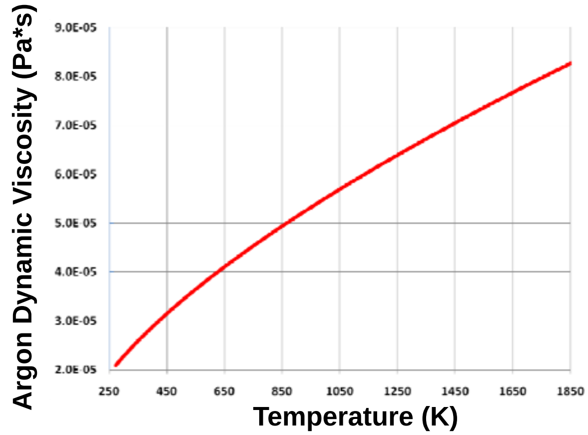

Ref:
*R. Dawe and E. Smith. Viscosity of Argon at High Temperatures. Science, Vol. 163, pp 675~676, 1969.

Porous Gas-flow Model (FLUENT)

Validation with 1-D Benchmark Problem

considering thermal effects on both argon permeability and gas expansion

B.C. for Case 1, fixed pressure:

$r=R_1$, $P=P_1$, $T=T_1$; $r=R_2$, $P=P_2$, $T=T_2$.

R_1 (m)	R_2 (m)	P_1 (Pa)	P_2 (Pa)
0.0375	0.0725	100000	200000

V_{inlet} (m/s)	T_1 (K)	T_2 (K)
0.0073	1800	1000

60000 cells

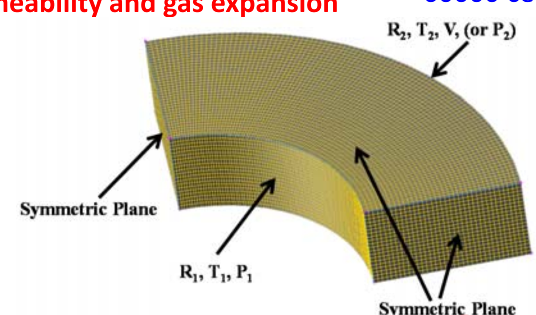

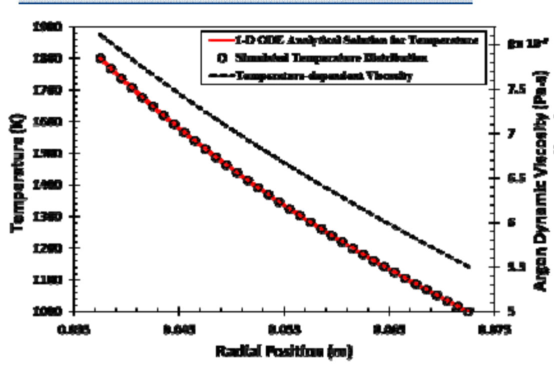

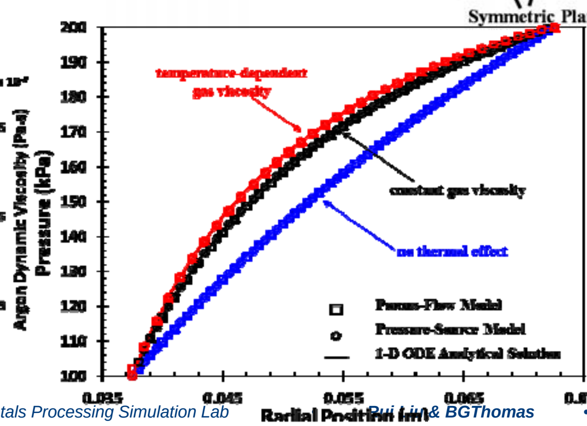

Pressure Threshold for Bubble Formation

- In order for gas to enter the liquid and form bubbles, interfacial surface tension force must be overcome:

Bubble expanding stage (assume equilibrium):

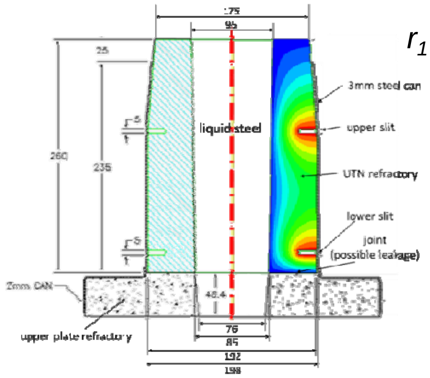

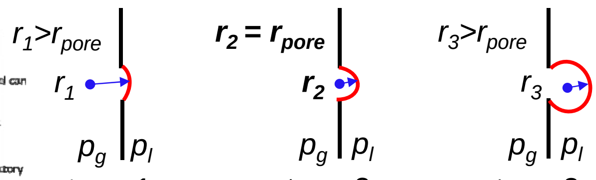

Pressure threshold for bubble formation:

$$p_g = p_l + \frac{2\sigma}{r}$$

r_{pore} has:

Smallest radius

Largest curvature

Biggest pressure drop

= critical condition

Parameters used in current study: $\boxed{\sigma = 1.2\, N/m \quad , \quad r_{pore} = 200\,\mu m}$

One-Way Flow Pressure Boundary Condition

At refractory-liquid interface: $(1-a(\mathbf{x}))\frac{\partial p(\mathbf{x})}{\partial n} + a(\mathbf{x})p(\mathbf{x}) = a(\mathbf{x})g(\mathbf{x})$

$$a(\mathbf{x}) = \frac{1 - sgn(\left(\frac{\partial p(\mathbf{x})}{\partial n}\right)_b)}{2} \qquad g(\mathbf{x}) = p_l(\mathbf{x}) + \frac{2\sigma}{r_{pore}} \qquad p_l = p_0 + \rho_l g\left(h_{tundish} + h_{UTN} - z\right) - \frac{1}{2}\rho_l U^2$$

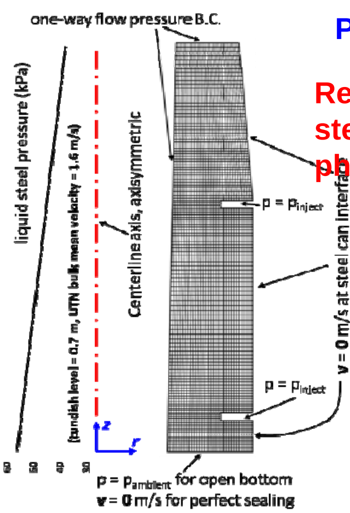

Pressure B.C. with $g(x)$

Reversed flow from the steel side, results not physical

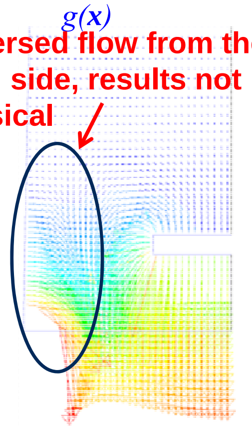

One-way flow pressure B.C.

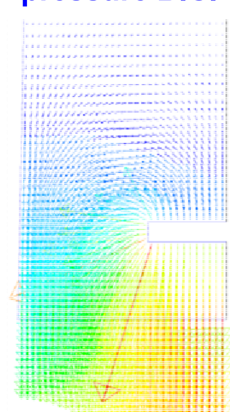

Gas Velocity (m/s)

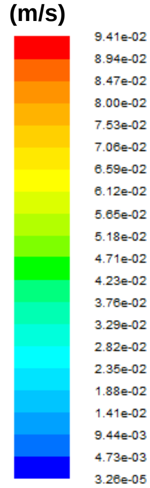

Effect of Injection Pressure

Gas velocity increases and distribution changes with increasing injection pressure:

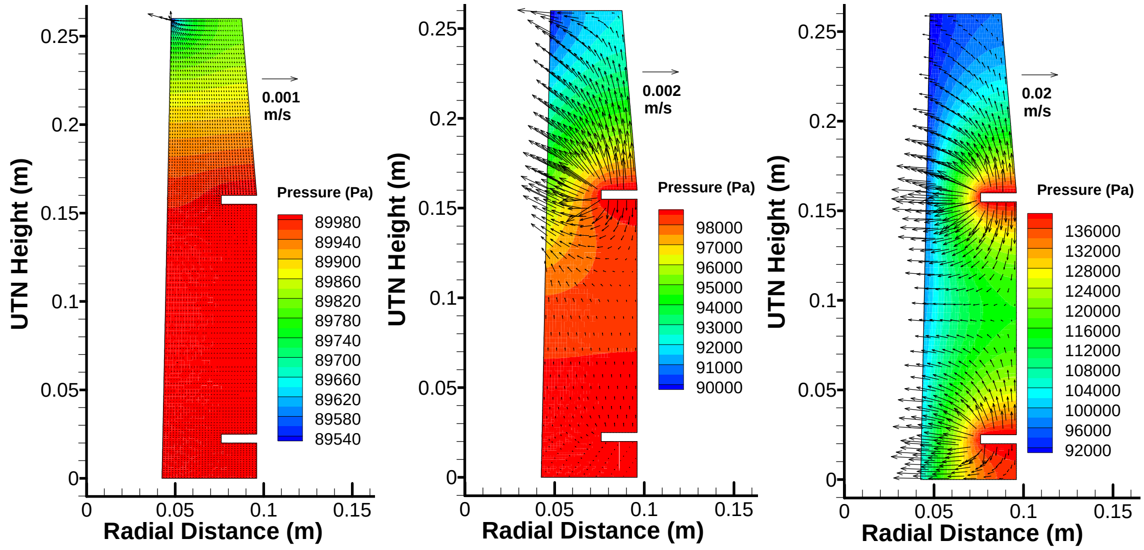

Injection pressure: **90 kPa** **110 kPa** **140 kPa**

Note: gas bubbles enter steel only where the threshold is overcome

Validation with Lab Experiment

Bubble Distribution on UTN Inner Surface

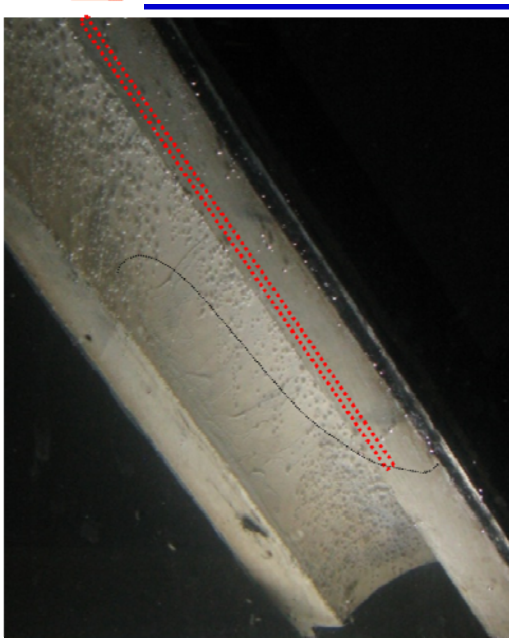

Measured preferential bubbling locations

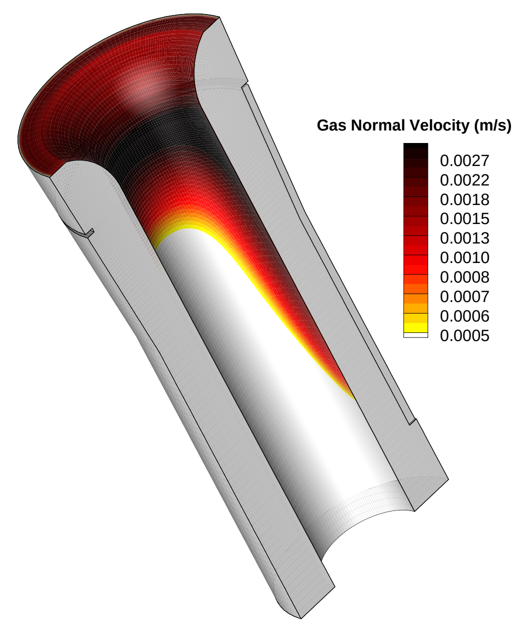

Predicted gas normal velocity distribution

Effect of nozzle thermal conductivity

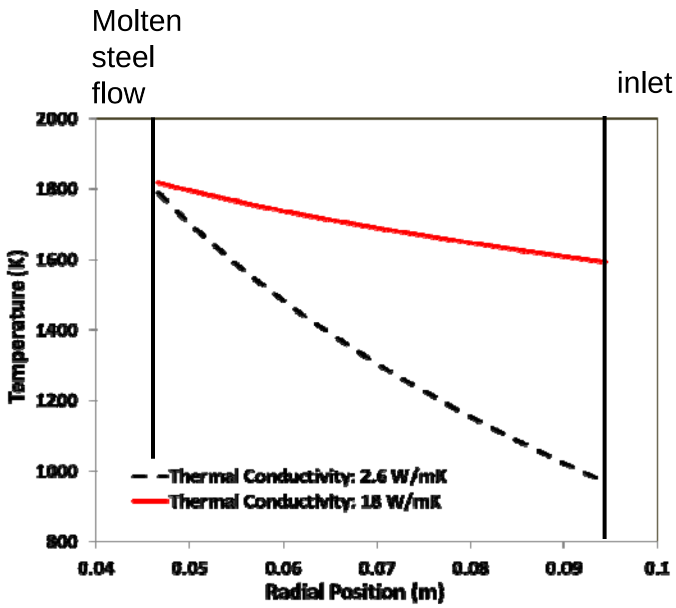

Decreasing conductivity (eg. by less graphite, or different refractory oxide such as doloma) causes:
- Higher temperature gradient
- Lower temperature near inlet
- Lower average nozzle temperature

Parametric study: Gas velocity profiles along UTN

Effects of: bottom leakage, pressure threshold, refractory conductivity

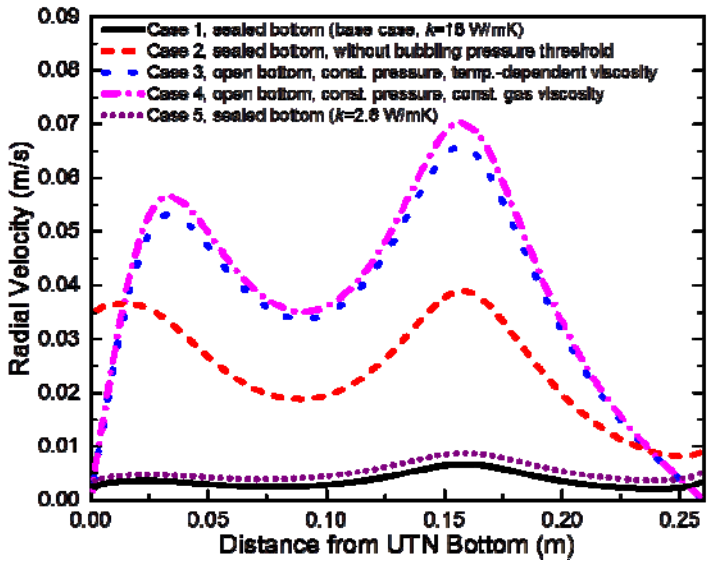

Base case:
- Max flow where slits are closest to UTN inner surface

Decreasing conductivity:
- Steepens temp. gradient
- Lowers inlet T & viscosity (higher permeability)
- Increases flow 30% (net)

Ignoring pressure threshold:
- increases flow (unrealistic)

Bottom seal leakage:
- Greatly increases flow everywhere (to keep constant pressure: otherwise pressure drops, revealing leakage)

Gas flow changes can greatly affect mold flow and quality

Initial Bubble Size Prediction

(Lee et al.,[1] 2010)

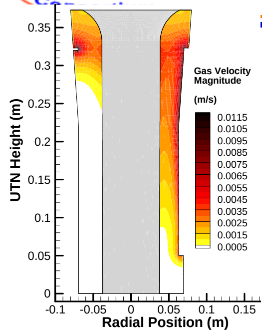

$$\text{Active sites per unit area}\,(\#/\text{cm}^2) = 7 \times \frac{Q_g^{0.2635} \times U^{0.85} \times P_{erm}^{0.3308}}{Radians(\theta)}$$

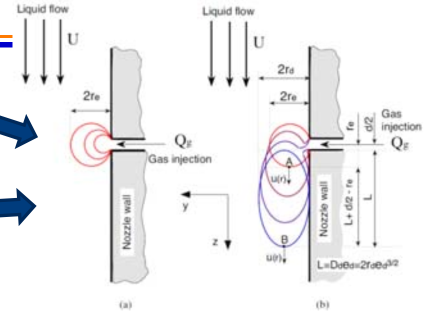

(Bai and Thomas,[2] 2001)

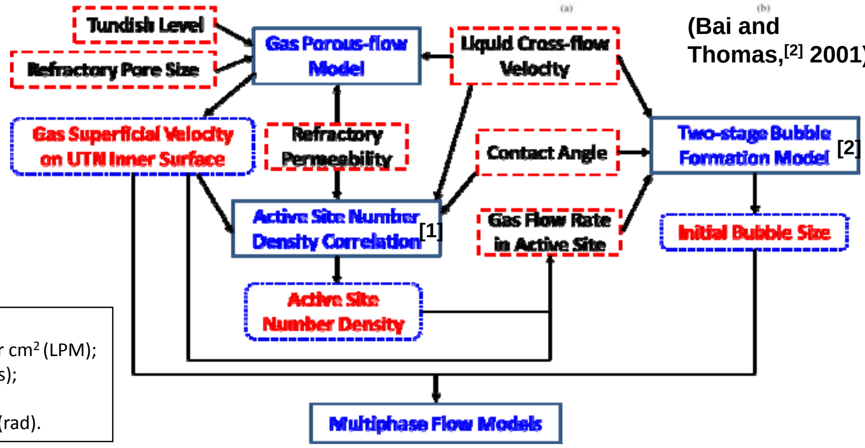

Ref:
[1] G. Lee, B.G. Thomas, et al., Met. Mater. Int., Vol. 16, No. 3 (2010), pp. 501~506

[2] H. Bai and B. G. Thomas, Metall. Mater. Trans. B 32, 1143(2001).

Where:
Q_g: the gas injection flow rate per cm² (LPM);
U: liquid superficial velocity (m/s);
P_{erm}: material permeability (npm);
θ: contact angle for wettability (rad).

Estimation of Active Sites Number at UTN Refractory Inner Surface

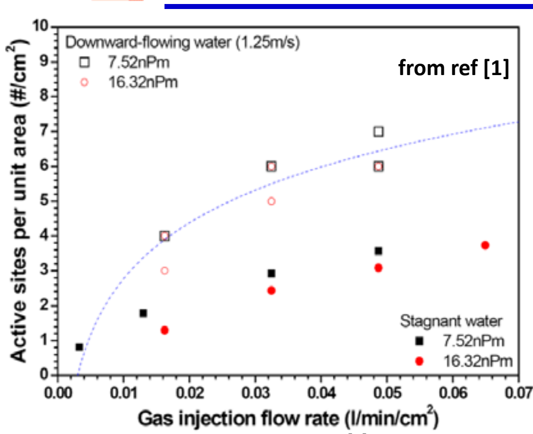

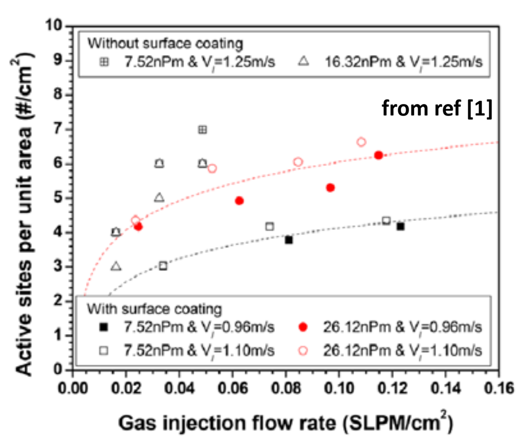

G. Lee and B.G. Thomas suggest[1]:

$$\text{Active sites per unit area}\,(\#/\text{cm}^2) = 7 \times \frac{Q_g^{0.2635} \times U^{0.85} \times P_{erm}^{0.3308}}{Radians(\theta)}$$

Where:
Q_g: the gas injection flow rate per cm² (LPM);
U: liquid superficial velocity (m/s);
P_{erm}: material permeability (npm);
ϑ: contact angle for wettability (rad)

So the number of active sites per cm² is:

$$N_{site} = \frac{7 Q_g^{0.2635} U^{0.85} P_{erm}^{0.3308}}{\theta}$$

Ref:
[1] G. Lee, B.G. Thomas, et al., Met. Mater. Int., Vol. 16, No. 3 (2010), pp. 501~506

Estimation of Mean Bubble Size using a Two-Stage Model

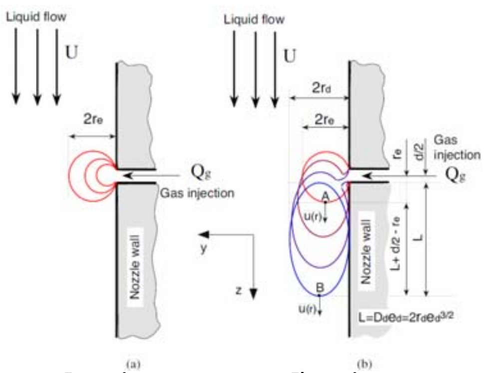

Expansion stage Elongation stage

--Figures from ref [2]

Active sites function as drilled holes where gas is injected. So based on the number of active sites and gas flow rate over an area, the gas flow rate per active site can be determined.

Ref:
[2] H. Bai and B. G. Thomas, Metall. Mater. Trans. B 32, 1143(2001).

Hua Bai's two-stage initial bubble formation model[2]:

1. **Expansion stage (solving for *r*, as r_e)**

$$\boxed{C_D \frac{1}{2}\rho_l \bar{u}^2 \pi r^2 = \frac{4}{3}\pi r^3(\rho_l-\rho_g)g + \frac{1}{2}\pi r\sigma \sin\theta_o(\cos\theta_r - \cos\theta_a)}$$

Drag coefficient: $C_D = \frac{24}{\mathrm{Re}_{bub}}(1+0.15\,\mathrm{Re}_{bub}^{0.687}) + 0.42/(1+4.25\times10^4\,\mathrm{Re}_{bub}^{-1.16})$

Bubble Reynolds number: $Re_{bub} = \frac{\bar{u}D}{\upsilon}$

$$\bar{u} = \frac{1}{2r}\int_{y=0}^{y=2r} u\,dy = 1.3173U\frac{r^{1/7}}{D_N^{1/7}}$$

Based on the 1/7th law in turbulent flow in the circular pipe

Contact angle function: $f_\theta = \sin\theta_o(\cos\theta_r - \cos\theta_a)$

$f\theta(U) = -0.06079 + 0.33109U(m/s) + 0.078773U(m/s)^2$

Empirical correlation with liquid steel superficial velocity

2. **Elongation stage (solving for r_d)**

$$\boxed{5.2692\frac{\pi U}{Q_g D_N^{1/7}}\int_{r_e}^{r_d}\left(r^{15/7}(ar+b)^{3/2} + \frac{ar^{22/7}}{2}(ar+b)^{1/2}\right)dr = 2r_d e_d^{3/2} + \frac{d}{2} - r_e}$$

$a = \frac{e_d - 1}{r_d - r_e}$ $b = \frac{r_d - e_d r_e}{r_d - r_e}$ $e_d = 0.78592 + 0.70797U(m/s) - 0.12793U(m/s)^2$

D_N :nozzle inner diameter (m)
ρ_l :liquid density (kg/m³)
ρ_g :gas density (kg/m³)
U :liquid steel superficial velocity (m/s)
σ :surface tension (N/m)
υ :kinematic viscosity of liquid steel (Pa*s)

Model 1

Flow Rate Prediction – Stopper-position-based Model

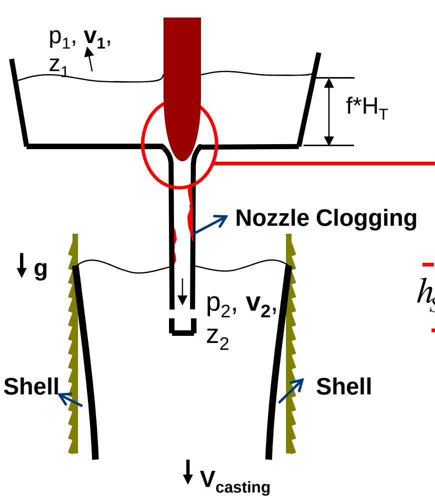

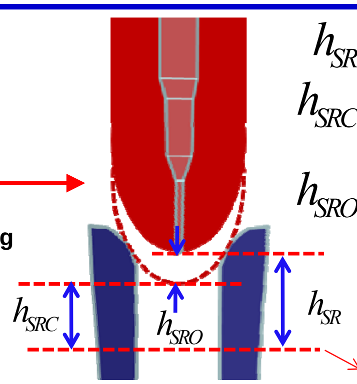

h_{SR} : **Stopper Rod Position**

h_{SRC} : **Stopper Rod Zero-Flow Position (closed position)**

h_{SRO} : **Stopper Rod Opening**

$$\boxed{h_{SRO} = h_{SR} - h_{SRC}}$$

Variables	Physical Meaning
h_{sen_sub}	SEN submergence depth
$f_{tundish}$	Tundish (weight) fraction
$h_{tundish}$	Total height of the tundish
L_{sen}	Distance from tundish bottom to SEN port center

Bernoulli's Equation: sub-model 2 sub-model 1 sub-model 3

$$\frac{p_1}{\rho g} + z_1 + \frac{V_1^2}{2g} = \frac{p_2}{\rho g} + z_2 + \frac{V_2^2}{2g} + h_{minor} + h_{friction} + h_{clogging}$$

$$Q_{SEN} = A_{SEN}\left(\frac{2g\left(f_{tundish}h_{tundish} - h_{sen\_sub} + L_{SEN}\right)}{1+0.5\left(\frac{A_{SEN}}{C_2 h_{SRO}^2}\right)^2 + \left(\frac{A_{SEN}}{C_2 h_{SRO}^2} - 1\right)^2 + C_1\frac{L_{SEN}}{D_{SEN}} + C_3}\right)^{0.5}$$

-- APPENDIX 1: Stopper-based model for SEN flow rate calculation

Sub-Model 1 – Modeling Friction Head Loss

Original Bernoulli's equation:

$$\frac{V_{SEN}^2}{2g}+h_{\text{gap}}+h_{\text{friction}}+h_{\text{clogging}}=-h_{\text{sen\_sub}}+f_{\text{tundish}}h_{\text{tundish}}+L_{\text{SEN}}$$

The friction head loss along the nozzle is modeled as:

$$h_{\text{friction}}=C_1\frac{L_{SEN}}{D_{SEN}}\frac{V_{SEN}^2}{2g}$$

***C_1* is a function of *Re* if SEN length and diameter are fixed**

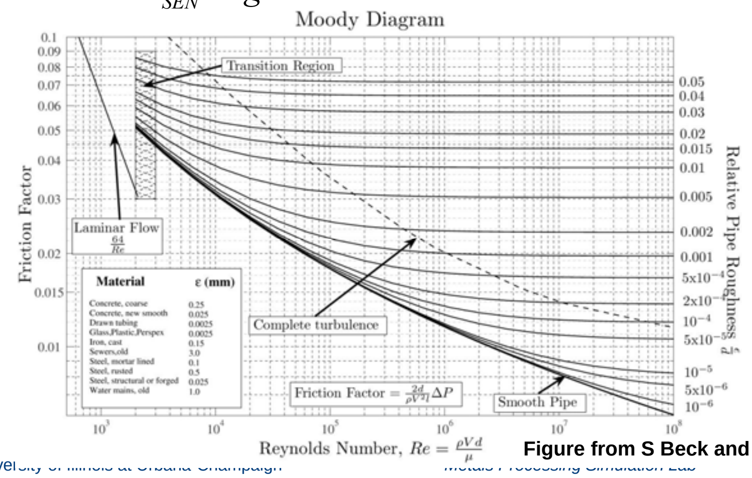

Figure from S Beck and R Collins, University of Sheffield

Since:

1.
Flow in the SEN usually reaches the *Re* of 10^5;

2.
The SEN inner surface is not smooth (due to attachment of the alumina oxide inclusions)

$$\boxed{C_1=0.07\sim0.08}$$

Sub-Model 2 – Modeling Stopper Rod Gap Minor Loss

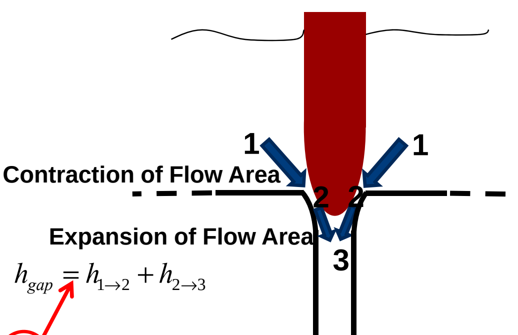

$$h_{gap}=h_{1\to2}+h_{2\to3}$$

$$\frac{V_{SEN}^2}{2g}+h_{\text{gap}}+h_{\text{friction}}+h_{\text{clogging}}=-h_{\text{sen\_sub}}+f_{\text{tundish}}h_{\text{tundish}}+L_{\text{SEN}}$$

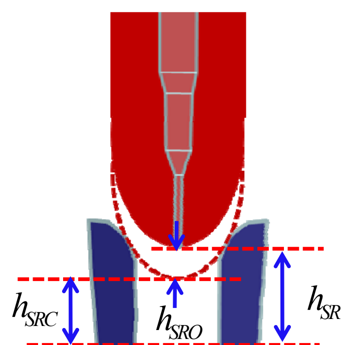

Assume: $\boxed{A_2=C_2h_{SRO}^2}$

Minor Loss in Contraction Case (reference [1]), from location 1 to location 2:

$$h_{1\to2}=\xi_{1\to2}\frac{V_2^2}{2g}\qquad \frac{A_2}{A_1}\to0\quad\Rightarrow\quad\boxed{\xi_{1\to2}=0.5}$$

$$\boxed{h_{gap}=h_{1\to2}+h_{2\to3}=\frac{V_{SEN}^2}{2g}\left[0.5\left(\frac{A_{SEN}}{C_2h_{SRO}^2}\right)^2+\left(\frac{A_{SEN}}{C_2h_{SRO}^2}-1\right)^2\right]}$$

Minor Loss in Expansion Case (reference [1]), from location 2 to location 3:

A_2, V_2 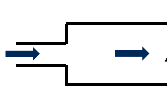 ***A_3, V_3***

$$h_{2\to3}=\xi_{2\to3}\frac{V_3^2}{2g}\qquad\boxed{\xi_{2\to3}=\left(\frac{A_3}{A_2}-1\right)^2}$$

Reference [1]:
Z. Zhang, G. Cui. Fluid Mechanics. Tsinghua University. 2005. ISBN: 7-302-03168-1/O201. pp330.

Final Form of SEN Flow Rate Q_{SEN} from Stopper-based Model

According to the friction head loss and loss models:

$$\frac{V_{SEN}^2}{2g}+h_{\text{gap}}+h_{\text{friction}}+h_{\text{clogging}}=-h_{\text{sen\_sub}}+f_{\text{tundish}}h_{\text{tundish}}+L_{\text{SEN}}$$

$$\frac{V_{SEN}^2}{2g}\left\{1+0.5\left(\frac{A_{SEN}}{C_2h_{SRO}^2}\right)^2+\left(\frac{A_{SEN}}{C_2h_{SRO}^2}-1\right)^2+C_1\frac{L_{SEN}}{D_{SEN}}\right\}+h_{\text{clogging}}=-h_{\text{sen\_sub}}+f_{\text{tundish}}h_{\text{tundish}}+L_{\text{SEN}}$$

Let $h_{\text{clogging}}=C_3\dfrac{V_{SEN}^2}{2g}$

$$\frac{V_{SEN}^2}{2g}\left\{1+0.5\left(\frac{A_{SEN}}{C_2h_{SRO}^2}\right)^2+\left(\frac{A_{SEN}}{C_2h_{SRO}^2}-1\right)^2+C_1\frac{L_{SEN}}{D_{SEN}}+C_3\right\}=-h_{\text{sen\_sub}}+f_{\text{tundish}}h_{\text{tundish}}+L_{\text{SEN}}$$

$$V_{SEN}=\sqrt{\frac{2g\left(-h_{\text{sen\_sub}}+f_{\text{tundish}}h_{\text{tundish}}+L_{\text{SEN}}\right)}{1+0.5\left(\frac{A_{SEN}}{C_2h_{SRO}^2}\right)^2+\left(\frac{A_{SEN}}{C_2h_{SRO}^2}-1\right)^2+C_1\frac{L_{SEN}}{D_{SEN}}+C_3}}$$

The model consists of three parameters,
C_1 for friction loss along the nozzle
C_2 for minor loss at stopper rod gap
C_3 for head loss due to clogging

$$\boxed{Q_{SEN}=A_{SEN}\sqrt{\frac{2g\left(-h_{\text{sen\_sub}}+f_{\text{tundish}}h_{\text{tundish}}+L_{\text{SEN}}\right)}{1+0.5\left(\frac{A_{SEN}}{C_2h_{SRO}^2}\right)^2+\left(\frac{A_{SEN}}{C_2h_{SRO}^2}-1\right)^2+C_1\frac{L_{SEN}}{D_{SEN}}+C_3}}}$$

Validation of Stopper-position-based Model

$$\boxed{Q_{SEN}=A_{SEN}\sqrt{\frac{2g\left(-h_{\text{sen\_sub}}+f_{\text{tundish}}h_{\text{tundish}}+L_{\text{SEN}}\right)}{1+0.5\left(\frac{A_{SEN}}{C_2h_{SRO}^2}\right)^2+\left(\frac{A_{SEN}}{C_2h_{SRO}^2}-1\right)^2+C_1\frac{L_{SEN}}{D_{SEN}}+C_3}}}$$

The model consists of three parameters,
C_1 for friction loss along the nozzle
C_2 for minor loss at stopper rod gap
C_3 for head loss due to clogging

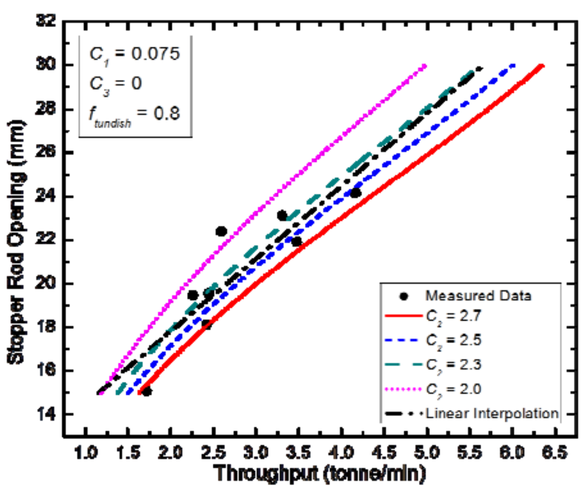

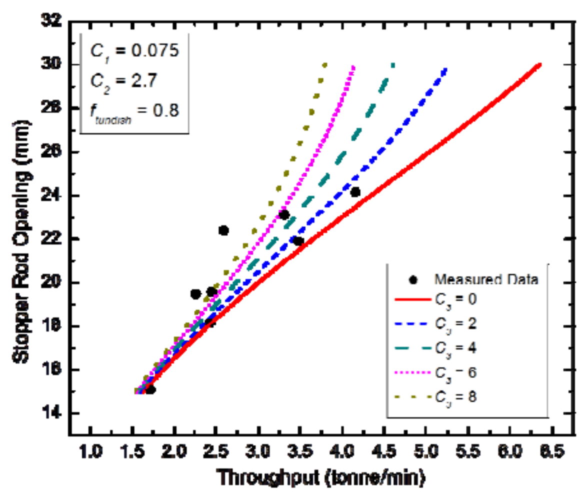

Modeling SEN Flow Rate

--Analysis of Bernoulli's Equation

$$\frac{p_0}{\rho g}+\frac{v_0^2}{2g}+z_0=\frac{p_3}{\rho g}+\frac{v_3^2}{2g}+z_3+h_{port}+h_f+h_{sg}$$

$$p_0=1.01\times10^5\,Pa$$

$$p_3=\rho g H_3+p_0$$

$$z_0-z_3=H_1+H_2+H_3$$

0

$$\frac{p_0-p_3}{\rho g}+z_0-z_3=\frac{v_3^2}{2g}+\sum h \rightarrow h_{port}+h_f+h_{sg}$$

$$-H_3 \qquad H_1+H_2+H_3 \qquad \frac{v_{SEN}^2}{2g}\left(\frac{A_{SEN}}{A_{port}}-1\right)^2 \qquad f\,\frac{L_{SEN}}{D_{SEN}}\frac{v_{SEN}^2}{2g}$$

$$\boxed{h_{sg}=\left(\left(\frac{1}{\mu}-1\right)^2\left(\frac{A_{SEN}}{A_{GAP}}\right)^2+\left(\frac{A_{SG}}{A_{GAP}}-\frac{A_{GAP}}{A_{SG}}\right)^2\left(\frac{A_{SEN}}{A_{SG}}\right)^2\right)\frac{v_{SEN}^2}{2g}}$$

$$\mu=\frac{A_{vc}}{A_{SG}}=\begin{cases}0.63+0.37\left(\frac{A_{GAP}}{A_{SG}}\right)^3 & \textbf{correlation 1[1]}\\ 0.5864+0.2762\left(\frac{A_{GAP}}{A_{SG}}\right)-0.4807\left(\frac{A_{GAP}}{A_{SG}}\right)^2+0.618\left(\frac{A_{GAP}}{A_{SG}}\right)^3 & \textbf{cor. 2[2]}\\ 0.64 & \textbf{cor. 3[3]}\end{cases}$$

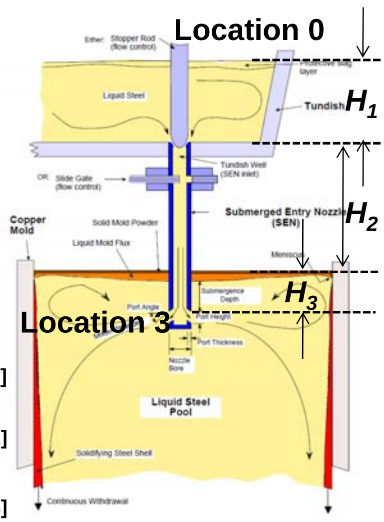

Ref:

[1] Oertel, Herbert; Prandtl, Ludwig, et.al, Prandtl's Essentials of Fluid Mechanics, Springer, ISBN 0387404376. See pp. 163–165.

[2] Evangelista Torricelli, 1643; [3] http://en.wikipedia.org/wiki/Vena_contracta

Slide-gate-position-based Model

Equation for gate-position-based model (including gas effect):

$$Q_{SEN}=A_{eff}\sqrt{\frac{2g\left(H_1+H_2\right)}{\left(\frac{A_{SEN}}{A_{port}}-1\right)^2+f\,\frac{L_{SEN}}{D_{SEN}}+\left(\frac{1}{\mu}-1\right)^2\left(\frac{A_{SEN}}{A_{GAP}}\right)^2+\left(\frac{A_{SG}}{A_{GAP}}-\frac{A_{GAP}}{A_{SG}}\right)^2\left(\frac{A_{SEN}}{A_{SG}}\right)^2+\left(\frac{A_{SEN}}{2A_{port}}\right)^2}}$$

where $\mu=0.63+0.37\left(\dfrac{A_{GAP}}{A_{SG}}\right)^3$

$$A_{eff}=\begin{cases}A_{SEN} & \text{single phase flow}\\ \dfrac{V_c WT}{Q_{gas}+V_c WT}A_{SEN} & \text{two phase flow}\end{cases}$$

For continuous caster, an extra term should be added to account for pressure drop due to clogging:

$$Q_{SEN}=A_{eff}\sqrt{\frac{2g\left(H_1+H_2\right)}{\left(\frac{A_{SEN}}{A_{port}}-1\right)^2+f\,\frac{L_{SEN}}{D_{SEN}}+\left(\frac{1}{\mu}-1\right)^2\left(\frac{A_{SEN}}{A_{GAP}}\right)^2+\left(\frac{A_{SG}}{A_{GAP}}-\frac{A_{GAP}}{A_{SG}}\right)^2\left(\frac{A_{SEN}}{A_{SG}}\right)^2+\left(\frac{A_{SEN}}{2A_{port}}\right)^2+C}}$$

In current study, *C=0* is assumed (no clogging).

Validation of Gate-position-based Model (Gate Position vs. Flow Rate)

- **Nice match obtained, analytical SEN flow rate model is validated**
- **Gap area is:**

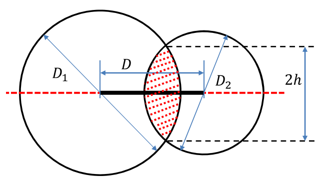

$$h = \frac{D_1 D_2}{4D}\sqrt{1-\left(\frac{D_1^2+D_2^2-4D^2}{2D_1D_2}\right)^2}$$

$$A_{GAP} = \frac{D_1^2}{4}\arcsin\left(\frac{2h}{D_1}\right)+\frac{D_2^2}{4}\arcsin\left(\frac{2h}{D_2}\right)-Dh, \quad if \quad D>\frac{\sqrt{D_1^2-D_2^2}}{2}$$

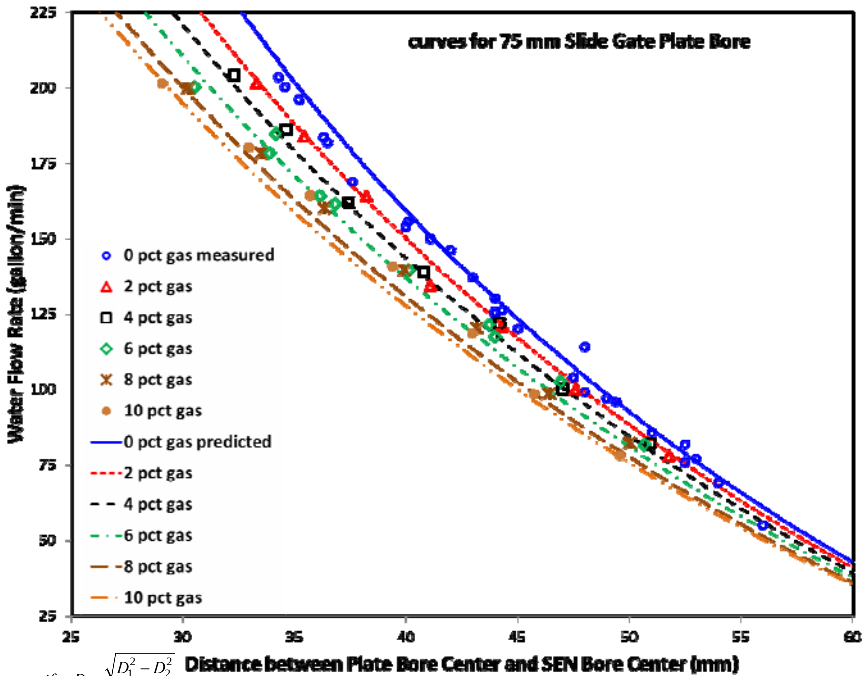

Average Mold Level Equation (AMLE)

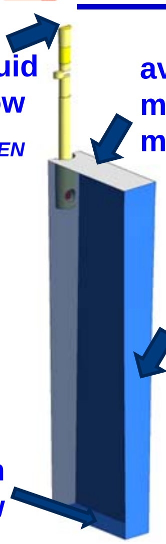

$$V_l\left(A_l-\frac{\pi}{4}D_o^2\right)+V_cA_l=Q_{SEN} \qquad A_l=WT$$

$$V_l=\frac{dh}{dt}$$

$$\frac{dh}{dt}=\frac{Q_{SEN}}{\alpha_A A_l}-\frac{V_c}{\alpha_A}$$

$$\alpha_A=1-\frac{\pi D_o^2}{4WT}$$

$$h=\int_{t_0}^{t}\left(\frac{Q_{SEN}}{\alpha_A A_l}-\frac{V_c}{\alpha_A}\right)dt'+h_0=\frac{1}{\alpha_A A_l}\int_{t_0}^{t}Q_{SEN}\,dt'-\frac{1}{\alpha_A}V_c\left(t-t_0\right)+h_0$$

Discretize the equation above in the time domain, resulting in the following form:

$$h_n=\frac{1}{\alpha_A A_l}\sum_{i=0}^{n}Q_{SEN}\left(t_i\right)\Delta t-\frac{1}{\alpha_A}V_c\left(t_n-t_0\right)+h_0$$

$$Q_{SEN}=A_{eff}\sqrt{\frac{2g\left(H_1+H_2\right)}{\left(\frac{A_{SEN}}{A_{port}}-1\right)^2+f\frac{L_{SEN}}{D_{SEN}}+\left(\frac{1}{\mu}-1\right)^2\left(\frac{A_{SEN}}{A_{GAP}}\right)^2+\left(\frac{A_{SG}}{A_{GAP}}-\frac{A_{GAP}}{A_{SG}}\right)^2\left(\frac{A_{SEN}}{A_{SG}}\right)^2+\left(\frac{A_{SEN}}{2A_{port}}\right)^2}}$$

Validation of AMLE model

--*with mold level measurements from ArcelorMittal 3 SP*

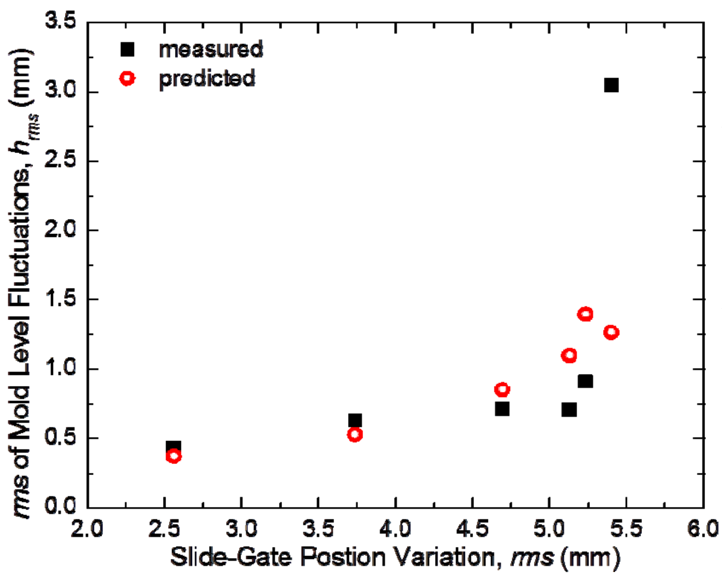

$$h_{rms} = \sqrt{\overline{h'^2}} = \sqrt{\frac{\sum_{i=1}^{N}\left(h_i - \bar{h}\right)^2}{N}}$$

- **Monotonic correlation found between flow rate variation and mold level fluctuations**
- **Mold level fluctuation deviates from the correlation when dithering frequency is very close to sloshing frequency of the mold (0.92 Hz in current case)**

Flow Rate Histories and Initial Bubble Size

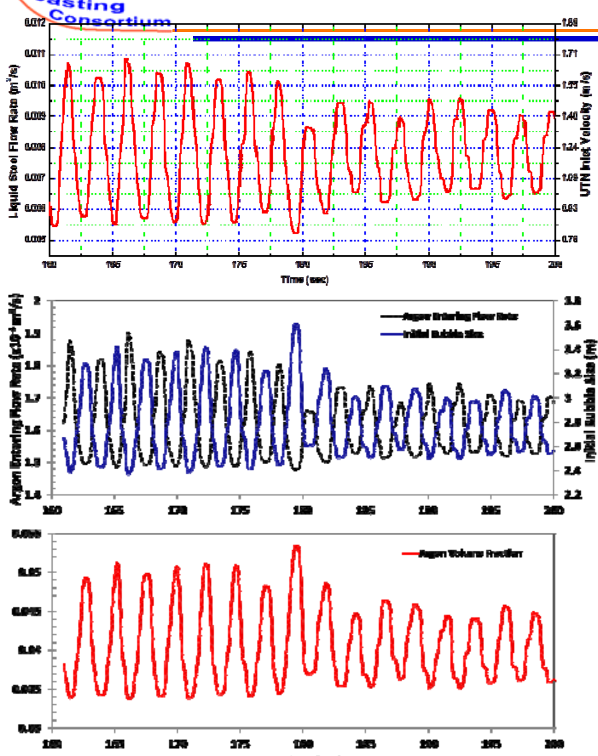

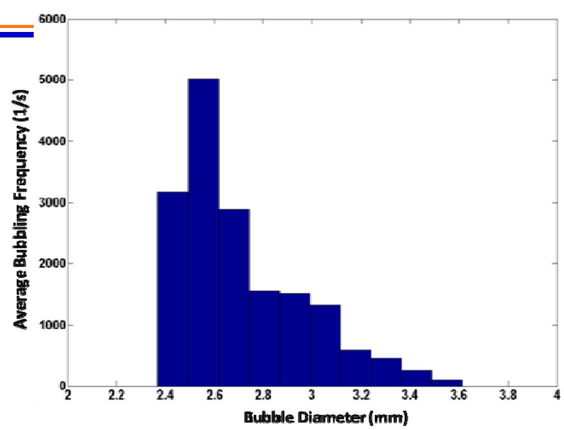

- **Increase in cross-flow velocity leads to increasing gas flow rate;**
- **Gas flow rate increase leads to increase in bubble size, and cross-flow velocity increase reduces bubble size. The net effect results in decrease of bubble size.**
- **Mean bubble size is used in simulation.**

Sloshing Case: Flow Pattern Evolution at Mold Center Plane

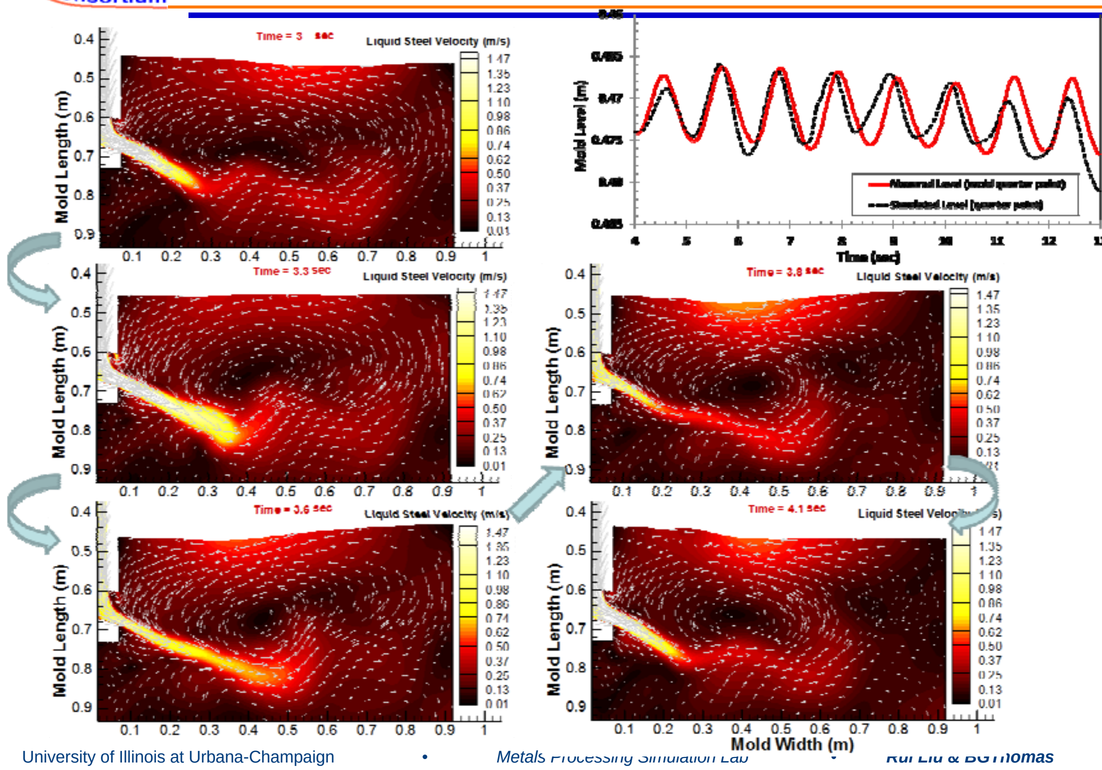

Mold Top Surface Level Variation -- Sloshing Case

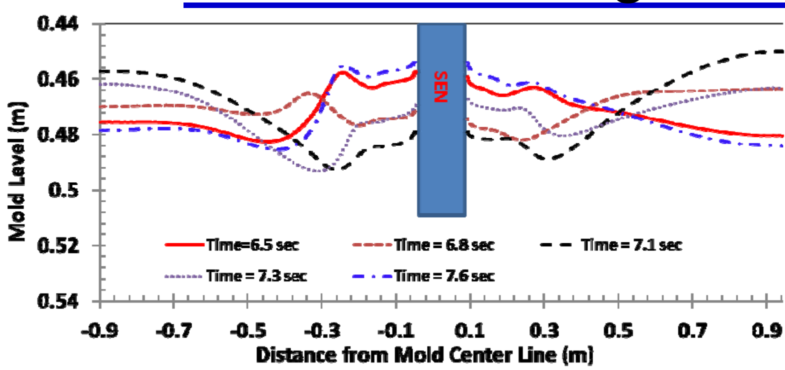

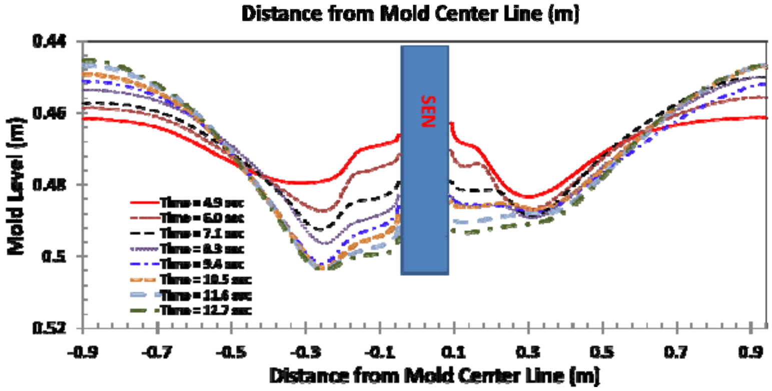

- Mold level sloshes mainly in the form of a standing wave across half mold;
- Traveling wave occurs near SEN towards narrow face;
- Sloshing amplitude increases with time at a decreasing rate.

Mold Level Fluctuation

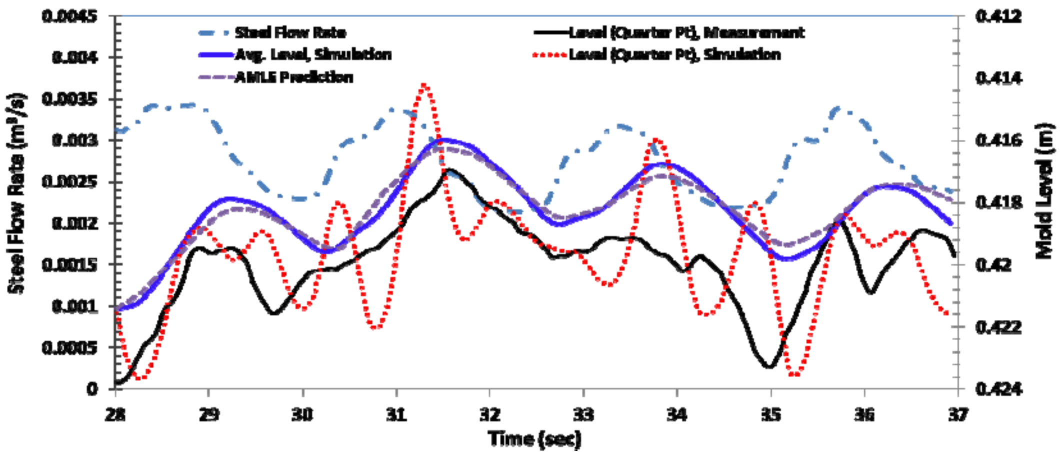

References

Modeling Transient Multiphase Flow and Mold Top Surface Behavior in Steel Continuous Casting
Rui Liu
PhD Thesis, University of Illinois, MechSE, 332p, 2014, CCC Report 201406

Model of Gas Flow through Porous Refractory Applied to an Upper Tundish Nozzle
Rui Liu and Brian G. Thomas
CCC Report 201402

Measurements of Molten Steel Surface Velocity and Effect of Stopper-rod Movement on Transient Multiphase Fluid Flow in Continuous Casting
Rui Liu, Brian G. Thomas, Joydeep Sengupta, Stephen D. Chung and ManhKha Trinh,
CCC Report 201401

Slidegate Dithering Effects on Transient Flow and Mold Level Fluctuations Iron and Steel Technology (reprint)
Liu, Rui, Brian G. Thomas, Love Kalra, Tathagata Bhattacharya, and Aloka Dasgupta Iron and Steel Technology, 11:7, July, 2014. (reprinted from AISTech 2013 Proceedings, Pittsburgh, PA, May 6-8, 2013, Assoc. Iron Steel Technology, Warrendale, PA, pp. 1351-1364)